

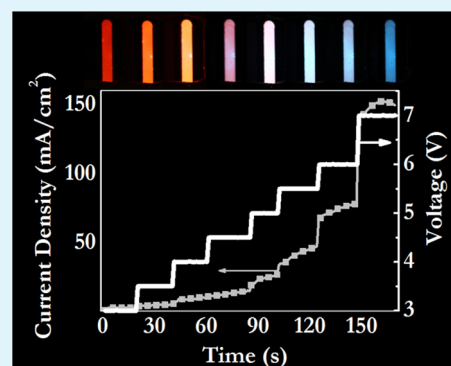
Combining an Ionic Transition Metal Complex with a Conjugated Polymer for Wide-Range Voltage-Controlled Light-Emission Color

Jia Wang,[†] Shi Tang,^{†,‡} Andreas Sandström,[‡] and Ludvig Edman^{*,†,‡}[†]The Organic Photonics and Electronics Group, Umeå University, SE-901 87 Umeå, Sweden[‡]LunaLEC AB, Tvistevägen 47, SE-907 19 Umeå, Sweden

Supporting Information

ABSTRACT: We report on voltage-controlled electroluminescence (EL) over a broad range of colors from a “two-luminophor” (2L) light-emitting electrochemical cell (LEC), comprising a blend of a majority blue-emitting conjugated polymer (blue-CP), a minority red-emitting ionic transition metal complex (red-iTMC), and an ion-transporting compound as the active layer. The EL color is reversibly shifted from red, over orange, pink, and white, to blue by simply changing the applied voltage from 3 to 7 V. An analysis of our results suggests that the low concentration of immobile cations intrinsic to this particular device configuration controls the electron injection and thereby the EL color: at low voltage, electrons are selectively injected into the low-barrier minority red-iTMC, but with increasing voltage the injection into the high-barrier majority blue-CP is gradually improved.

KEYWORDS: light-emitting electrochemical cell, tunable color, conjugated polymer, ionic transition metal complex, white emission, charge injection



1. INTRODUCTION

For a manifold of emissive applications, including high- and low-information content displays and signage as well as mood-controlled illumination, it is fundamental to be able to shift or tune the emission color from a pixel or an entire device on-demand during operation. One notable success story in this aspect is the organic light-emitting diode (OLED), which recently was commercially introduced as the high-information content display in various high-end applications such as cellular phones and digital cameras.^{1,2} However, the fabrication of OLEDs and similar display-fit technologies (e.g., the inorganic LED and the liquid crystal display) is technically challenging and expensive, and the interest for alternative low-cost technologies capable of achieving an on-demand control of the light-emission color is significant.^{3,4}

An easy-to-fabricate and low-cost alternative to the OLED is the light-emitting electrochemical cell (LEC),^{5–8} but such devices commonly feature solely monochrome emission.^{9–11} A few exceptions do however exist in the literature. Yang and Pei¹² reported on a bias-direction dependent electroluminescence (EL) color from a bilayer LEC: when biased at one polarity, the bilayer LEC emitted green light (from one layer), and when biased with the opposite polarity, it emitted orange light (from the other layer). A similar bias-direction dependent EL color was reported by De Cola and co-workers¹³ a few years later. These authors employed a blend of a poly(*para*-phenylenevinylene) derivative and a dinuclear ruthenium complex as the active layer and showed that such devices emit red EL at forward bias (+4 V) and green EL at reverse bias

(−4 V). Finally, Dumur and co-workers¹⁴ report on a time-dependent change of the emission color from green to yellow from an LEC comprising a cationic iridium complex as the emitter. They attributed the temporal change of the emission color to a temperature-induced modification of either the molecular packing or to a degradation of the active layer.

Here, we report that it is possible to control the EL color from a single-layer LEC, from red, over orange, pink, and white, to blue, by increasing the applied voltage from 3 to 7 V in small steps. The forward-bias control of the EL color over such a wide range is effectuated through the employment of a carefully tuned single-layer LEC, comprising two distinctly different luminophors and an ion-transporting compound as the active layer. Through the employment of complementary measurements and model formulation, we demonstrate that the voltage-controlled EL color most plausibly is effectuated by the existence of a low concentration of immobile cations at the cathodic interface in this particular device configuration.

2. EXPERIMENTAL SECTION

The active material in our 2L-LECs comprises a blend of a blue-emitting poly spirofluorene-based conjugated copolymer (“blue-CP”, Merck, catalogue number SPB-02T), a red-emitting ionic transition metal complex tris[4,4'-di-*tert*-butyl-(2,2')-bipyridine]ruthenium(II) (PF₆)₂ (“red-iTMC”, Luminescence Technology Corporation), and ion-conducting poly(ethylene oxide) (PEO, $M_w = 5 \times 10^6$ g/mol,

Received: November 13, 2014

Accepted: January 9, 2015

Published: January 9, 2015

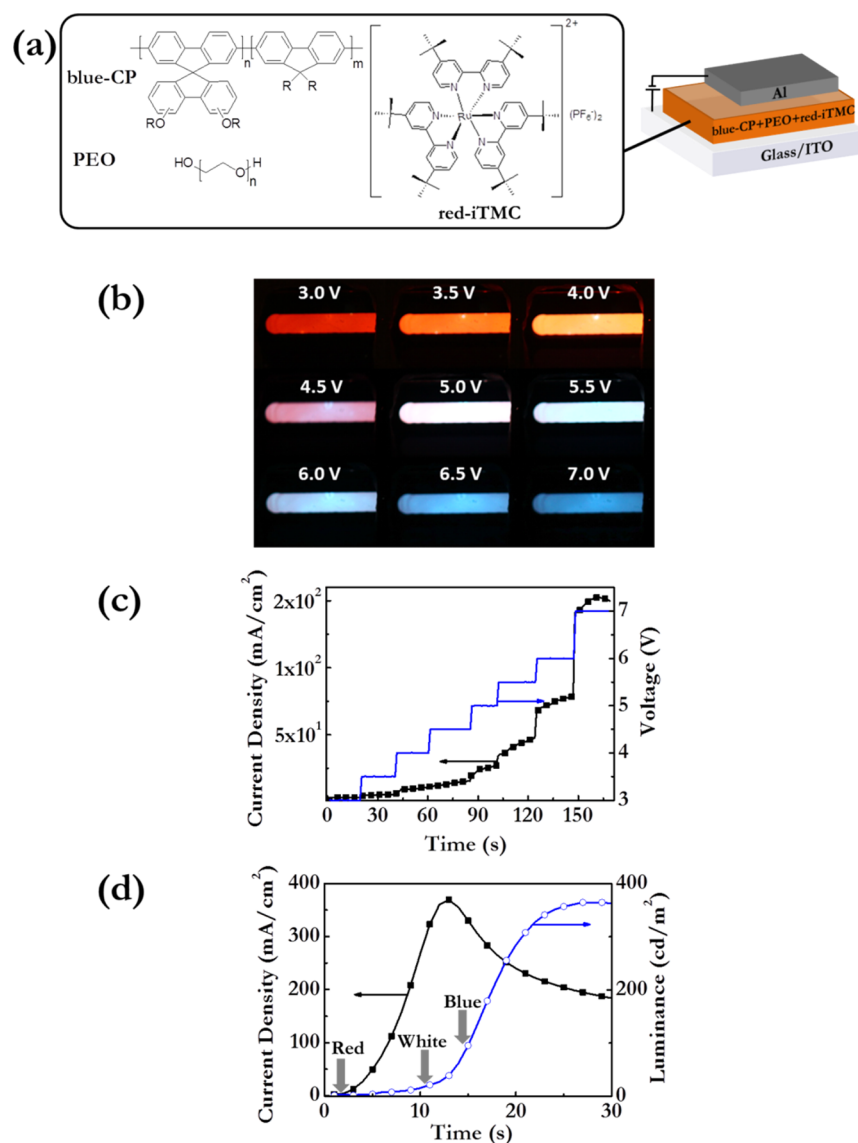


Figure 1. (a) The device structure of the two-luminophor light-emitting electrochemical cell (2L-LEC), with the chemical structure of the constituent materials in the active material depicted in the left inset. (b) Time-lapse photographs of the light-emission, and (c) the corresponding current density–voltage–time graph, following a number of consecutive voltage steps. (d) The temporal evolution of the current density and luminance for a 2L-LEC during constant-voltage driving at 7 V, with the gray arrows indicating the starting point of three of the different colors.

Sigma-Aldrich). The chemical structures are displayed in the left inset of Figure 1a.

The active-material constituents were separately dissolved in chloroform (anhydrous, Sigma-Aldrich) in a 10 mg/mL concentration, and thereafter blended in a mass ratio of [blue-CP:red-iTMC:PEO] = [1:0.2:0.1]. Other mass ratios were also tested but resulted in a lowered device performance. The active-material solution was spin-coated (spin speed = 1000 rpm, $t = 60$ s) onto a carefully cleaned indium–tin oxide (ITO) coated glass substrate (Thin Film Devices), where after the active-material film (dry thickness = 78 nm) was annealed on a hot plate ($T = 323$ K, $t = 3$ h). A set of four Al cathodes were thermally evaporated ($p < 2 \times 10^{-4}$ Pa) onto the active layer through a shadow mask; the size of the cathode defined the emission area as 0.85×0.15 cm². The device structure is schematically depicted in Figure 1a.

The LEC devices were characterized using a computer-controlled source-measure unit (Agilent U2722A) and a calibrated photodiode equipped with an eye-response filter (Hamamatsu Photonics) connected to a data acquisition card (National Instruments USB-6009) via a current-to-voltage amplifier. All device preparations and measurements were performed at $T = 298$ K under inert atmosphere

in two interconnected N₂-filled glove boxes ([O₂], [H₂O] <1 ppm). The energy levels of the active-material constituents were estimated with cyclic voltammetry (CV), using a procedure described in detail previously.¹⁵ The PL spectra were recorded with a spectrometer (LS-55, PerkinElmer), equipped with a Xe discharge lamp (pulse power = 20 kW, pulse duration = 8 μ s) and two monochromators (Monk-Gillieson); the excitation wavelength was 360 nm (blue-CP and 2L-blend) or 460 nm (red-iTMC). The EL spectra were recorded with a fiber-optic spectrometer (USB2000, Ocean Optics).

3. RESULTS AND DISCUSSION

LECs commonly comprise either a conjugated polymer (CP),^{16–20} or an ionic transition metal complex (iTMC),^{21–28} as the luminescent species (“the luminophor”), but for the purpose of voltage-controlled emission-color, we utilize a two-luminophor LEC (2L-LEC).²⁹ The two luminophores are distinctly different in that the blue-CP is an ion-free, hydrophobic, large-energy-gap, singlet-emitting semiconductor, whereas the red-iTMC is an ionic, relatively

hydrophilic, small-energy-gap, triplet-emitting semiconductor which features mobile (PF_6^-) anions. For the attainment of the desired phenomena of a voltage-tunable emission color, it was necessary to make the blue-CP the majority luminophor and the red-iTMC the minority luminophor. The PEO functions as a compatibilizer between the two luminophores, and the attainment of an optically clear active-material film required the inclusion of PEO. PEO also assists in transporting the PF_6^- anions in the active material during device operation, as, e.g., manifested in that PEO-free 2L-LECs featured a much higher drive voltage.

Figure 1b displays the broad range of stabilized emission colors, red, orange, pink, white, and blue, emitted by the 2L-LEC during an increase in voltage from 3 to 7 V in discrete steps of 0.5 V. Following such a voltage step, it typically took 5–10 s before the complete shift to the new emission color had been effectuated. Figure 1c presents the corresponding current density–voltage–time graph, and we note that the current also exhibits a temporal change, i.e., an increase, following a voltage step, and that the new color stabilizes faster than the current.

Figure 1d reveals that the 2L-LEC features the characteristic signs of LEC operation, i.e., an increasing current and luminance with time during potentiostatic driving. These data were collected at 7 V, but the same qualitative trend was observed at lower drive voltages of 3 and 5 V. This implies that the 2L-LEC indeed is a functional LEC, which features electric double layer formation, electrochemical doping, and the in situ formation of a p–n junction doping structure.^{30–33} The same color-shift sequence, red → orange → pink → white → blue, as observed during the voltage-step experiments in Figure 1c, was detected also during the potentiostatic driving at 7 V; some of the onset times at which the emission colors were first observed are indicated by gray arrows in Figure 1d. At a lower applied voltage, the spectrum of the color palette decreased; at 5 V, red, orange, pink, and white EL could be detected, whereas at 3 V solely red emission was observed. The corresponding EL spectra as a function of time are presented in Figures S1–S3 in the Supporting Information. As the color-change process is found to be repeatable in both the voltage-step and potentiostatic experiments, we can exclude irreversible morphological changes and side reactions as the enabling factor. Information on the optoelectronic properties at the different drive voltages are presented in Table S1 in the Supporting Information.

We now attempt to explain the mechanism behind the color-changing phenomenon in the 2L-LEC. Figure 2a presents the device energetics at open circuit, specifically the HOMO and LUMO levels of the red-iTMC luminophor (dashed red lines) and the blue-CP luminophor (solid blue lines) as well as the work functions of the two electrodes. We note that a charge-transfer exciton, an exciplex, with the electron positioned on the red-iTMC and the hole on the blue-CP, is an energetically favorable species that can form during operation of a 2L-LEC. If such an exciplex is luminescent, it will feature a red-shifted emission as compared to the red-iTMC.

Figure 2b displays PL spectra of solid-state films comprising the red-iTMC, the blue-CP, and the 2L-LEC active layer. The PL spectrum of the 2L-LEC film is essentially identical to that of the blue-CP, and distinctly different from the red-iTMC film. The conclusion must then be that the energy transfer from the blue-CP majority component to the red-iTMC minority component in the 2L-LEC, in the form of Förster transfer and/or singlet-exciton diffusion, is inefficient. In other words,

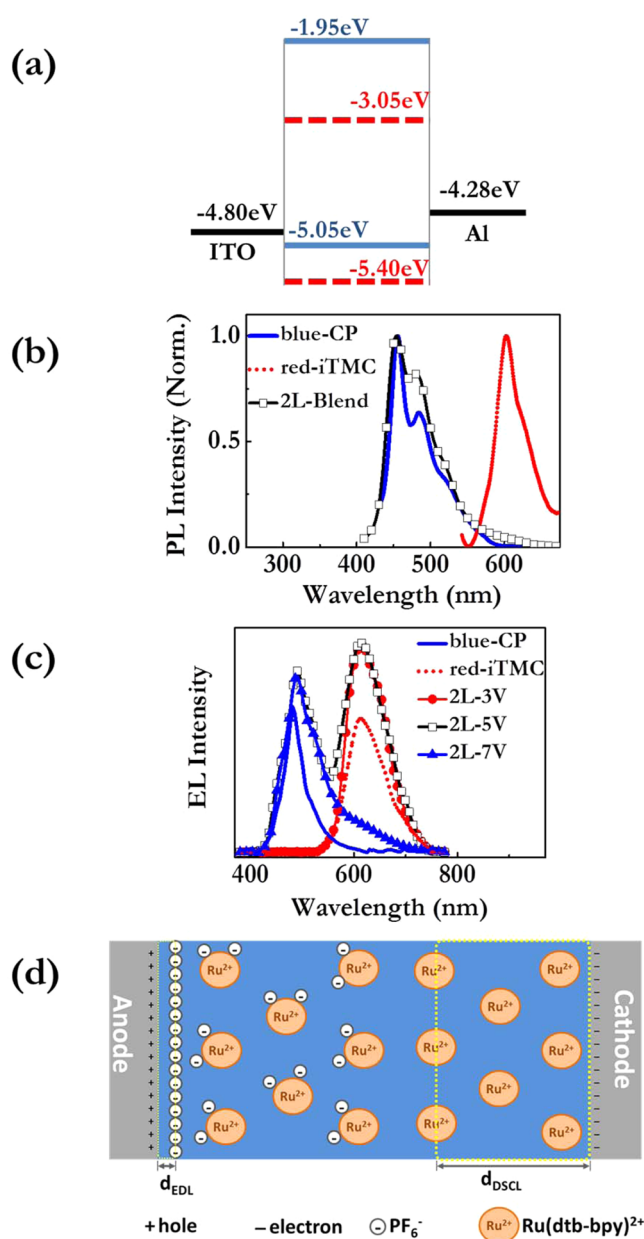


Figure 2. (a) Energy levels of the 2L-LEC at open circuit, with the dashed red lines representing the red-iTMC and the solid blue lines representing the blue-CP. (b) Normalized PL spectra from a red-iTMC film, a blue-CP film, and a 2L-Blend film. (c) EL spectra from a red-iTMC 1L-LEC (driven at 3.2 V), a blue-CP 1L-LEC (driven at 4.0 V), and a 2L-LEC at 3 different drive voltages: 3.0, 5.0, and 7.0 V. Note that the EL spectra from the 1L-LECs have been downshifted for clarity. (d) A schematic illustrating the electric double layer at the anodic interface and the dispersed space charge layer next to the cathodic interface.

the 2L-LEC does not function as a host–guest system.³⁴ Moreover, if exciplexes are formed in the 2L-LEC active layer during optical excitation, these are dark.

Figure 2c presents the EL spectra from a red-iTMC 1L-LEC (driven at 3.2 V) and a blue-CP 1L-LEC (driven at 4.0 V), as well as the stabilized EL spectra from the 2L-LEC at three different drive voltages of 3, 5, and 7 V. The EL peak of the red-iTMC and the blue-CP 1L-LECs are positioned at 611 and 482 nm, respectively. We find that the EL spectrum of the 2L-LEC at the low voltage of 3 V [EL peak = 614 nm, CIE coordinates:

(0.63, 0.36)] is highly similar to that of the red-iTMC, but that with increasing voltage, the contribution of the higher-energy blue-CP becomes gradually more important. At the intermediate voltage of 5 V, the contributions from the two luminophores are approximately identical, as manifested in two similarly sized EL peaks at 614 and 490 nm and the attainment of white light emission with CIE coordinates of (0.40, 0.38), a correlated color temperature (CCT) of 3500 K, and a color rendering index (CRI) of 59. At the high voltage of 7 V, the EL spectrum of the 2L-LEC [EL peak = 490 nm, CIE coordinates: (0.23, 0.39)] is dominated by the blue-CP, although a minor low-energy tail also can be distinguished. As this tail is not distinguishably red-shifted in comparison to the red-iTMC, it is again confirmed that potential exciplexes are dark. Moreover, as the EL from the 2L-LEC is effectively a superposition of the EL from the two constituent luminophores, with a gradual shift from the low-energy red-iTMC to the high-energy blue-CP with increasing voltage, the conclusion is that potential interluminophor interactions are weak or absent.

The kinetic aspect of the EL color change, i.e., the characteristic “slow” change of the emission color in the constant-voltage experiments (see Figure 1d), implies that ion redistribution, and not solely electronic processes, plays a key role in the color-shift process. Further evidence to this end is provided by the ion-mobility-impaired PEO-free devices, which only featured (uneven) red emission at a high voltage of 8 V following a long turn-on time of >1000 s. An interesting question in this context then relates to why the 2L-LEC does not emit blue EL from the majority constituent at low voltage? More specifically, LEC devices are conventionally described and demonstrated to allow for EL at the thermodynamic limit, i.e., at $V = E_g/e$;^{35–37} so why is an applied voltage of 3 V not sufficient for the realization of blue EL from the 2L-LEC?

It is at this stage appropriate to call attention to that it is only the small PF_6^- anion that is mobile in the active layer of the 2L-LEC, whereas the large and bulky $\text{Ru}(\text{dtb-bpy})^{2+}$ cation is effectively immobile. During the initial device operation, the mobile PF_6^- anions will drift and accumulate within a thin “electric double layer” (EDL) at the anode, and a rough approximation of the width of this EDL is provided by the van der Waals radius of the PF_6^- anion, $d_{\text{EDL}} \approx R_{\text{PF}_6} = 0.26 \text{ nm}$.³⁸

During the EDL formation process, the drifting PF_6^- anions will leave uncompensated $\text{Ru}(\text{dtb-bpy})^{2+}$ cations in a “dispersed space charge layer” (DSCL) at the cathode. On the basis of the large size and immobility of the cations, it is to be expected that the DSCL has a larger effective width (d_{DSCL}), over which the electrostatic potential drops, than the EDL. In this context, we emphasize that conventional 1L-LECs based on an iTMC as the single luminophor commonly are observed to turn on and begin to emit light at or close to the energy-gap potential^{39,40} but that our manifestation of the 2L-LEC features an important distinguishing feature in that the ion concentration is significantly lower, as the ionic red-iTMC species is diluted by the blue-CP and the PEO so that it only amounts to 15 mass % (this ion-concentration difference is further amplified by the common procedure of adding an ionic liquid to the active material in conventional iTMC-based 1L-LECs.⁴¹) Thus, it is reasonable to anticipate that $d_{\text{DSCL}} \gg d_{\text{EDL}}$ for the 2L-LEC, as schematically outlined in Figure 2d.

A rough quantitative value for d_{DSCL} is provided by estimating the effect of the anion-free cations by squeezing them all into a thin layer at a distance from the cathode corresponding to half the thickness of the DSCL:

$$d_{\text{cation}} = d_{\text{DSCL}}/2 \quad (1)$$

The voltage drop between this thin ionic layer and the cathode can be calculated by using a rearrangement of the double-plate capacitor equation:

$$\Delta V = \Delta Q \times d_{\text{cation}} / (\epsilon_r \times \epsilon_0 \times A) \quad (2)$$

where ΔQ and ϵ_r are the uncompensated cationic charge and the dielectric constant in the DSCL, respectively, ϵ_0 is the vacuum permittivity, and A is the cross sectional area. ΔQ is further accessible as

$$\Delta Q = e \times A \times d_{\text{DSCL}} \times n_{\text{cat,DSCL}} \quad (3)$$

where e is the elementary charge and $n_{\text{cat,DSCL}}$ is the cationic concentration in the DSCL region. The latter is given by

$$n_{\text{cat,DSCL}} = \rho_{\text{iTMC,AM}} \times N_A / M_{\text{iTMC}} \quad (4)$$

where $\rho_{\text{iTMC,AM}}$ is the density of the red-iTMC complex in the active material, N_A is Avogadro's constant, and M_{iTMC} is the molecular weight of the red-iTMC complex. Combining eqs 1–4, we get:

$$d_{\text{DSCL}} = [(2 \times \epsilon_r \times \epsilon_0 \times M_{\text{iTMC}}) / (e \times \rho_{\text{iTMC,AM}} \times N_A)]^{0.5} \times (\Delta V)^{0.5} \quad (5)$$

By setting $\rho_{\text{iTMC,AM}} = 0.15 \text{ g/cm}^3$ and $\epsilon_r = 5$ and using tabulated values for the other parameters, we obtain

$$d_{\text{DSCL}} = 2.7 \times 10^{-9} \times (\Delta V)^{0.5} \quad (6)$$

Figure 2a provided information on the barrier heights for electron (hole) injection from the Al cathode (ITO anode) into the two luminophores. These values correspond to the lowest potential drops over the cathodic interface at which electronic injection can take place, but if the corresponding barrier widths, as estimated by d_{DSCL} in eq 6, are large, it is very plausible that a larger potential drop is needed. The barrier height for electron injection into the red-iTMC is 1.23 eV, which corresponds to $d_{\text{DSCL}} = 3.0 \text{ nm}$, using eq 6. The barrier height for electron injection into the blue-CP is significantly larger at 2.33 eV, and it translates into $d_{\text{DSCL}} = 4.1 \text{ nm}$. It is notable that these values for d_{DSCL} are much larger than the value for $d_{\text{EDL}} \approx 0.26 \text{ nm}$, as provided previously. Moreover, at supernanometer distances, tunneling injection begins to be cumbersome. It is accordingly highly probable that a significant overpotential is required for the attainment of efficient electron injection into both the red-iTMC and the blue-CP, where the first barrier to be surmounted is that of the red-iTMC. Thus, the anticipated scenario is that electron injection into the minority red-iTMC and the accompanying red light emission is attained at low overpotentials but that electron injection into the majority blue-CP begins to be significant, and eventually dominant, with increasing overpotential. That is, the scenario that was observed experimentally in Figure 1. Note further that once electron and hole injection are effectuated, electrochemical doping and p–n junction formation will follow, as is the conventional scenario in a functional LEC.

4. CONCLUSION

To conclude, we present a 2-luminophor LEC, comprising a blend of a red-emitting ionic transition metal complex, a blue-emitting conjugated polymer, and a compatibilizing ion transporter sandwiched between two air-stable electrodes.

We demonstrate that a broad spectrum of emission colors can conveniently be selected from such a device through the applied potential. We finally argue that the voltage-controlled light-emission is effectuated by a low concentration of immobile cations at the cathodic interface, which is a unique feature of the selected device architecture.

■ ASSOCIATED CONTENT

■ Supporting Information

Information on the optoelectronic performance parameters of the 2L-LEC during potentiostatic driving is presented in tabular form. The temporal evolution of the current density, luminance, and EL spectra during biasing at 3, 5, and 7 V. This material is available free of charge via the Internet at <http://pubs.acs.org>.

■ AUTHOR INFORMATION

■ Corresponding Author

*E-mail: ludvig.edman@physics.umu.se.

■ Notes

The authors declare no competing financial interest.

■ ACKNOWLEDGMENTS

This project was financially supported by the Swedish Foundation for Strategic Research, Vetenskapsrådet, Energimyndigheten, and the Knut and Alice Wallenberg foundation. L.E. is a “Royal Swedish Academy of Sciences Research Fellow” supported by a grant from the Knut and Alice Wallenberg Foundation.

■ REFERENCES

- (1) Chandra, V. K.; Chandra, B. P.; Jha, P., Organic Light-Emitting Diodes and Their Applications. In *Luminescence: Basic Concepts, Applications and Instrumentation*; Virk, H. S., Ed.; Trans Tech Publications Ltd: Stafa-Zurich, 2014; Vol. 357, pp 29–93.
- (2) Mertens, R. *The OLED Handbook*; 1st ed; Metalgrass Software: Herzelia, Israel, 2011.
- (3) Sheats, J. R. Manufacturing and Commercialization Issues in Organic Electronics. *J. Mater. Res.* **2004**, *19*, 1974–1989.
- (4) Sondergaard, R. R.; Hosel, M.; Krebs, F. C. Roll-to-Roll Fabrication of Large Area Functional Organic Materials. *J. Polym. Sci., Part B: Polym. Phys.* **2013**, *51*, 16–34.
- (5) Liang, J. J.; Li, L.; Niu, X. F.; Yu, Z. B.; Pei, Q. B. Fully Solution-Based Fabrication of Flexible Light-Emitting Device at Ambient Conditions. *J. Phys. Chem. C* **2013**, *117*, 16632–16639.
- (6) Hernandez-Sosa, G.; Tekoglu, S.; Stolz, S.; Eckstein, R.; Teusch, C.; Trapp, J.; Lemmer, U.; Hamburger, M.; Mechau, N. The Compromises of Printing Organic Electronics: A Case Study of Gravure-Printed Light-Emitting Electrochemical Cells. *Adv. Mater.* **2014**, *26*, 3235–3240.
- (7) Sandstrom, A.; Asadpoorardavish, A.; Enevold, J.; Edman, L. Spraying Light: Ambient-Air Fabrication of Large-Area Emissive Devices on Complex-Shaped Surfaces. *Adv. Mater.* **2014**, *26*, 4975–4980.
- (8) Sandstrom, A.; Dam, H. F.; Krebs, F. C.; Edman, L. Ambient Fabrication of Flexible and Large-Area Organic Light-Emitting Devices Using Slot-Die Coating. *Nature Commun.* **2012**, *3*, 1002.
- (9) Pei, Q. B.; Yu, G.; Zhang, C.; Yang, Y.; Heeger, A. J. Polymer Light-Emitting Electrochemical Cells. *Science* **1995**, *269*, 1086–1088.
- (10) Matyba, P.; Andersson, M. R.; Edman, L. On the Desired Properties of a Conjugated Polymer-Electrolyte Blend in a Light-Emitting Electrochemical Cell. *Org. Electron.* **2008**, *9*, 699–710.
- (11) Lee, T. W.; Zausseil, J.; Kim, S. H.; Hsu, J. W. P. High-Efficiency Soft-Contact-Laminated Polymer Light-Emitting Devices with Patterned Electrodes. *Adv. Mater.* **2004**, *16*, 2040–2045.

(12) Yang, Y.; Pei, Q. B. Voltage Controlled Two Color Light-Emitting Electrochemical Cells. *Appl. Phys. Lett.* **1996**, *68*, 2708–2710.

(13) Welter, S.; Brunner, K.; Hofstra, J. W.; De Cola, L. Electroluminescent Device with Reversible Switching between Red and Green Emission. *Nature* **2003**, *421*, 54–57.

(14) Dumur, F.; Nasr, G.; Wantz, G.; Mayer, C. R.; Dumas, E.; Guerlin, A.; Miomandre, F.; Clavier, G.; Bertin, D.; Gignès, D. Cationic Iridium Complex for the Design of Soft Salt-Based Phosphorescent OLEDs and Color-Tunable Light-Emitting Electrochemical Cells. *Org. Electron.* **2011**, *12*, 1683–1694.

(15) Tang, S.; Mindemark, J.; Araujo, C. M. G.; Brandell, D.; Edman, L. Identifying Key Properties of Electrolytes for Light-Emitting Electrochemical Cells. *Chem. Mater.* **2014**, *26*, 5083–5088.

(16) Shoji, T. D.; Zhu, Z. H.; Leger, J. M. Characterizing Ion Profiles in Dynamic Junction Light-Emitting Electrochemical Cells. *ACS Appl. Mater. Interfaces* **2013**, *5*, 11509–11514.

(17) Inayeh, A.; Dorin, B.; Gao, J. Scanning Photocurrent and Photoluminescence Imaging of a Frozen Polymer p–n Junction. *Appl. Phys. Lett.* **2012**, *101*, 25.

(18) Tang, S.; Pan, J.; Buchholz, H.; Edman, L. White Light-Emitting Electrochemical Cell. *ACS Appl. Mater. Interfaces* **2011**, *3*, 3384–3388.

(19) Yu, Z.; Wang, M.; Lei, G.; Liu, J.; Li, L.; Pei, Q. Stabilizing the Dynamic P–I–N Junction in Polymer Light-Emitting Electrochemical Cells. *J. Phys. Chem. Lett.* **2011**, *2*, 367–372.

(20) Li, X.; Altal, F.; Liu, G.; Gao, J. Long-Term, Intermittent Testing of Sandwich Polymer Light-Emitting Electrochemical Cells. *Appl. Phys. Lett.* **2013**, *103*, 24.

(21) Meier, S. B.; Hartmann, D.; Winnacker, A.; Sarfert, W. The Dynamic Behavior of Thin-Film Ionic Transition Metal Complex-Based Light-Emitting Electrochemical Cells. *J. Appl. Phys.* **2014**, *116*, 10.

(22) Bolink, H. J.; Cappelli, L.; Coronado, E.; Gaviña, P. Observation of Electroluminescence at Room Temperature from a Ruthenium(II) Bis-terpyridine Complex and Its Use for Preparing Light-Emitting Electrochemical Cells. *Inorg. Chem.* **2005**, *44*, 5966–5968.

(23) Costa, R. D.; Ortí, E.; Bolink, H. J.; Monti, F.; Accorsi, G.; Armaroli, N. Luminescent Ionic Transition-Metal Complexes for Light-Emitting Electrochemical Cells. *Angew. Chem., Int. Ed.* **2012**, *51*, 8178–8211.

(24) Hu, T.; He, L.; Duan, L.; Qiu, Y. Solid-State Light-Emitting Electrochemical Cells Based on Ionic Iridium(III) Complexes. *J. Mater. Chem.* **2012**, *22*, 4206–4215.

(25) Bernhard, S.; Barron, J. A.; Houston, P. L.; Abruna, H. D.; Ruglovsky, J. L.; Gao, X.; Malliaras, G. G. Electroluminescence in Ruthenium(II) Complexes. *J. Am. Chem. Soc.* **2002**, *124*, 13624–13628.

(26) Rudmann, H.; Shimada, S.; Rubner, M. F. Solid-State Light-Emitting Devices Based on the Tris-Chelated Ruthenium(II) Complex. 4. High-Efficiency Light-Emitting Devices Based on Derivatives of the Tris(2,2'-bipyridyl) Ruthenium(II) Complex. *J. Am. Chem. Soc.* **2002**, *124*, 4918–4921.

(27) Slinker, J.; Bernards, D.; Houston, P. L.; Abruna, H. D.; Bernhard, S.; Malliaras, G. G. Solid-State Electroluminescent Devices Based on Transition Metal Complexes. *Chem. Commun.* **2003**, *19*, 2392–2399.

(28) Slinker, J. D.; Rivnay, J.; Moskowitz, J. S.; Parker, J. B.; Bernhard, S.; Abruna, H. D.; Malliaras, G. G. Electroluminescent Devices from Ionic Transition Metal Complexes. *J. Mater. Chem.* **2007**, *17*, 2976–2988.

(29) Sessolo, M.; Tordera, D.; Bolink, H. J. Ionic Iridium Complex and Conjugated Polymer Used to Solution-Process a Bilayer White Light-Emitting Diode. *ACS Appl. Mater. Interfaces* **2013**, *5*, 630–634.

(30) Pei, Q. B.; Yang, Y.; Yu, G.; Zhang, C.; Heeger, A. J. Polymer Light-Emitting Electrochemical Cells: In Situ Formation of a Light-Emitting p–n Junction. *J. Am. Chem. Soc.* **1996**, *118*, 3922–3929.

(31) Matyba, P.; Maturova, K.; Kemerink, M.; Robinson, N. D.; Edman, L. The Dynamic Organic p–n Junction. *Nature Mater.* **2009**, *8*, 672–676.

(32) Meier, S. B.; van Reenen, S.; Lefevre, B.; Hartmann, D.; Bolink, H. J.; Winnacker, A.; Sarfert, W.; Kemerink, M. Dynamic Doping in Planar Ionic Transition Metal Complex-Based Light-Emitting Electrochemical Cells. *Adv. Funct. Mater.* **2013**, *23*, 3531–3538.

(33) van Reenen, S.; Matyba, P.; Dzwilewski, A.; Janssen, R. A. J.; Edman, L.; Kemerink, M. Salt Concentration Effects in Planar Light-Emitting Electrochemical Cells. *Adv. Funct. Mater.* **2011**, *21*, 1795–1802.

(34) Gong, X.; Ostrowski, J. C.; Moses, D.; Bazan, G. C.; Heeger, A. J. Electrophosphorescence from a Polymer Guest–Host System with an Iridium Complex as Guest: Förster Energy Transfer and Charge Trapping. *Adv. Funct. Mater.* **2003**, *13*, 439–444.

(35) Qian, G.; Lin, Y.; Wantz, G.; Davis, A. R.; Carter, K. R.; Watkins, J. J. Saturated and Multi-Colored Electroluminescence from Quantum Dots Based Light Emitting Electrochemical Cells. *Adv. Funct. Mater.* **2014**, *24*, 4484–4490.

(36) Su, H. C.; Cheng, C. Y. Recent Advances in Solid-State White Light-Emitting Electrochemical Cells. *Isr. J. Chem.* **2014**, *54*, 855–866.

(37) Sandstrom, A.; Matyba, P.; Inganas, O.; Edman, L. Separating Ion and Electron Transport: The Bilayer Light-Emitting Electrochemical Cell. *J. Am. Chem. Soc.* **2010**, *132*, 6646–6647.

(38) Katsuta, S.; Imai, K.; Kudo, Y.; Takeda, Y.; Seki, H.; Nakakoshi, M. Ion Pair Formation of Alkylimidazolium Ionic Liquids in Dichloromethane. *J. Chem. Eng. Data* **2008**, *53*, 1528–1532.

(39) Hasan, K.; Donato, L.; Shen, Y. L.; Slinker, J. D.; Zysman-Colman, E. Cationic Iridium(III) Complexes Bearing Ancillary 2,5-Dipyridyl(pyrazine) (2,5-DPP) and 2,2':5',2''-Terpyridine (2,5-TPY) Ligands: Synthesis, Optoelectronic Characterization and Light-Emitting Electrochemical Cells. *Dalton Trans.* **2014**, *43*, 13672–13682.

(40) Nazeeruddin, M. K.; Weh, R. T.; Zhou, Z.; Klein, C.; Wang, Q.; De Angelis, F.; Fantacci, S.; Grätzel, M. Efficient Green–Blue Light-Emitting Cationic Iridium Complex for Light-Emitting Electrochemical Cells. *Inorg. Chem.* **2006**, *45*, 9245–9250.

(41) Parker, S. T.; Slinker, J. D.; Lowry, M. S.; Cox, M. P.; Bernhard, S.; Malliaras, G. G. Improved Turn-on Times of Iridium Electroluminescent Devices by Use of Ionic Liquids. *Chem. Mater.* **2005**, *17*, 3187–3190.